Am J Physiol Renal Physiol 308: F728–F736, 2015.
First published January 28, 2015; doi:10.1152/ajprenal.00409.2014.

MAD2B contributes to podocyte injury of diabetic nephropathy via inducing cyclin B1 and Skp2 accumulation

Hua Su,[1]* Qiang Wan,[2]* Xiu-Juan Tian,[1]* Fang-Fang He,[1] Pan Gao,[1] Hui Tang,[1] Chen Ye,[1] Di Fan,[1] Shan Chen,[1] Yu-Mei Wang,[1] Xian-Fang Meng,[3] and Chun Zhang[1]

[1]*Department of Nephrology, Union Hospital, Tongji Medical College, Huazhong University of Science and Technology, Wuhan, China;* [2]*Department of Nephrology, Shandong Provincial Hospital Affiliated to Shandong University, Jinan, China; and* [3]*Department of Neurobiology, School of Basic Medical Sciences, Tongji Medical College, Huazhong University of Science and Technology, Wuhan, China*

Submitted 22 July 2014; accepted in final form 19 January 2015

Su H, Wan Q, Tian X, He F, Gao P, Tang H, Ye C, Fan D, Chen S, Wang Y, Meng X, Zhang C. MAD2B contributes to podocyte injury of diabetic nephropathy via inducing cyclin B1 and Skp2 accumulation. *Am J Physiol Renal Physiol* 308: F728–F736, 2015. First published January 28, 2015; doi:10.1152/ajprenal.00409.2014.—It is well documented that mitotic arrest deficiency (MAD)2B can inhibit the anaphase-promoting complex/cyclosome (APC/C) via cadherin (Cdh)1 and, consequently, can destroy the effective mitotic spindle checkpoint control. Podocytes have been observed to rapidly detach and die when being forced to bypass cell cycle checkpoints. However, the role of MAD2B, a cell cycle regulator, in podocyte impairment of diabetic nephropathy (DN) is unclear. In the present study, we investigated the significance of MAD2B in the pathogenesis of DN in patients, an animal model, and in vitro podocyte cultures. By Western blot and immunohistochemistry analyses, we found that MAD2B was evidently upregulated under high glucose milieu in vivo and in vitro, whereas Cdh1 was inhibited with high glucose exposure. Overexpression of MAD2B in podocytes by plasmid DNA transfection suppressed expression of Cdh1 and triggered the accumulation of cyclin B1 and S phase kinase-associated protein (Skp)2, two key molecules involving in cell cycle regulation, and the subsequent podocyte insult. In contrast, MAD2B deletion alleviated the high glucose-induced reduction of Cdh1 as well as the elevation of cyclin B1 and Skp2, which rescued the podocyte from damage. Taken together, our data demonstrate that MAD2B may play an important role in high glucose-mediated podocyte injury of DN via modulation of Cdh1, cyclin B1, and Skp2 expression.

mitotic arrest deficiency 2B; diabetic nephropathy; podocytes; cyclin B1; S phase kinase-associated protein 2

DIABETIC NEPHROPATHY (DN) is one of the leading causes of chronic and end-stage renal disease in worldwide, and it has been studied extensively (20). The mesangial matrix expansion was believed to be the central lesion of DN. However, nowadays, accumulating evidence highly suggests that the podocyte is the cardinal player in the pathogenesis of DN (23, 29).

Podocytes, which line the outer aspect of the glomerular basement membrane (GBM), play a vital role in maintaining an intact size and charge barrier as well as the shape of the capillary loop (21). Normally, as a terminally differentiated cell, the podocyte is unable to proliferate and renew; therefore, it cannot be effectively repaired or replaced. Once podocytes are lost to a certain extent, this leads to capillary tuft abnormality and glomerulosclerosis. Reduction of podocyte number is a strong predictor of progressive renal disease. It is well known that high glucose can interfere with podocyte cell-cell interactions, its attachment to the GBM, and apoptosis (1, 22). In particular, podocyte apoptosis is strongly associated with the onset of hyperglycemia in type 1 and type 2 diabetes models (24). Nevertheless, the precise mechanism mediating podocyte damage under hyperglycemia has not been fully clarified.

It has been reported that certain pathological stimuli can induce podocytes to reenter into the cell cycle; however, a terminally differentiated podocyte cannot complete its replication and maintain its actin cytoskeleton during mitosis (15). Consequently, at the end of mitosis, cytoskeletal actins form part of a contractile ring, leading to the rounding of podocytes, which results in podocyte detachment or death. The orderly mitotic events are regulated by the anaphase-promoting complex/cyclosome (APC/C), a large multiprotein E3 ubiquitin ligase that targets key mitotic regulators, such as cyclin B1 and S phase kinase-associated protein (Skp)2, for ubiquinitination and proteasomal degradation. Cadherin (Cdh)1 is one of the APC/C activating subunits that tightly controls APC/C activation. Cdh1-APC/C activation governs mitotic exit and G_1 phase maintenance, thus regulating the onset of DNA replication (7, 18, 27). Importantly, cyclin B1 and Skp2, two molecules actively involved in cell cycle control, are ubiquitinated by Cdh1-APC/C and then degraded (28, 30). Because of APC/C-Cdh1's critical role in cell cycle regulation, it probably links quiescent and mototic processes in most cell types (8, 13, 27). For example, in terminally differentiated neurons, it was found that Cdh1-APC/C attenuated cell-cycle progression and prevented S phase entry, via keeping cyclin B1 at a low level (2), whereas depletion of Cdh1 triggered cyclin B1-mediated entry into the S phase, which eventually led to neuron apoptosis (3).

Mitotic arrest deficiency (MAD)2B was originally identified as a member of the family of MAD genes and has been implicated in controlling the mitotic spindle checkpoint (5, 6, 19), which is important for the proper attachment of spindle microtubules to kinetochores during the metaphase-to-anaphase transition. It has been shown that MAD2B can directly interact with Cdh1 and inhibits Cdh1-mediated APC activation, thereby regulating the process of cell cycle, suggesting an important role for MAD2B in mitosis control (2, 6, 16, 19).

Since neurons and podocytes are both terminally differentiated cells, they likely have similar cell cycle control mechanisms. However, whether MAD2B and Cdh1-APC/C are involved in podocyte impairment induced by hyperglycemia still needs to be

* H. Su, Q. Wan, and X.-J. Tian contributed equally to this work.

Address for reprint requests and other correspondence: C. Zhang, Dept. of Nephrology, Union Hospital, Tongji Medical College, Huazhong Univ. of Science and Technology, 1277 Jie Fang Ave., Wuhan, Hubei 430022, China (e-mail: drzhangchun@hust.edu.cn).

elucidated. Here, we present new findings showing that under hyperglycemic conditions, MAD2B was upregulated, along with diminished Cdh1-APC/C abundance, and ultimately resulted in the accumulation of cyclin B1 and Skp2 as well as injury of podocytes, which was reversed by MAD2B depletion. Our results suggest that MAD2B-induced cyclin B1 and Skp2 accumulation can be implicated in podocyte injury in DN.

MATERIALS AND METHODS

Ethics statement. All animal experimental procedures and human renal biopsy samplings carried out in this study were approved by the Ethics Committee of Huazhong University of Science and Technology and were in compliance with guidelines for animal care set forth by this committee.

Human renal biopsy samples. Renal biopsies were performed as part of routine clinical diagnostic investigation. The patients' kidney tissue was sampled by the Department of Pathology, Wuhan Union Hospital. Control samples were obtained from the healthy kidney poles of individuals who underwent tumor nephrectomy without any primary or secondary renal diseases.

Animal samples. All experiments were performed in accordance with National Institutes of Health guidelines for the use and care of laboratory animals and were approved by the Animal Care and Use Committee of Tongji Medical College. Adult C57BL/6 mice, Sprague Dawley rats, and Wistar rats were provided by the Medical Experimental Animal Center of Tongji Medical College. Age-matched (12 wk) adult male C57BL/6J wild-type mice and homozygous leptin receptor-deficient *db*/*db* mice [B6.BKS(D)-Leprdb/J, stock no. 000697] were purchased from The Jackson Laboratories (Bar Harbor, ME). Animals were anesthetized with pentobarbital sodium before kidneys were removed. The renal cortex, medulla, and papilla were dissected at 4°C (26, 33). Glomeruli from the above-mentioned animals were isolated by the sieving method (31). Briefly, kidneys were flushed with ice-cold Krebs-Henseleit-saline buffer via an aortal catheter. The minced renal cortex was passed through three steel sieves (200, 120, and 80 mm) using ice-cold Krebs-Henseleit-saline buffer, and glomeruli were recovered from the 80-mm sieve, washed, and resuspended. Renal tubular cells were isolated by pressing fragments of the renal cortex through an 80-mesh screen and further enzymatic dissociation in vitro. Tissues were snap frozen in liquid nitrogen and stored at −80°C until extraction of total RNA or protein.

Cell cultures. Mouse kidney mesangial cells, rat tubular epithelial cells, and mouse glomerular endothelial cells were obtained from the American Type Culture Collection. Immortalized human podocyte cells (HPCs) were a gift from Dr. Heping Ma (Emory University). After cells became 70% confluence at 33°C, they were incubated at 37°C for 2 wk to allow differentiation before any experimental manipulations. Conditionally immortalized mouse podocytes (MPCs) were propagated at 33°C in DMEM containing 5 mM glucose, 10% FBS, 2 mM glutamine, 100 U/ml penicillin, 100 μg/ml streptomycin, 10 U/ml recombinant interferon (IFN)-γ. Once cells had reached 70–80% confluence, differentiation and a quiescent phenotype were induced by culture under nonpermissive conditions at 37°C without IFN-γ for 2 wk, resulting in disappearance of the T antigen. Mouse kidney mesangial cells were cultured in DMEM-F-12 (3:1) supplemented with 14 mM HEPES, 100 U/ml penicillin, 100 μg/ml streptomycin, and 5% FBS. Rat tubular epithelial cells were cultured in DMEM containing 10% FBS in saturated humidity and 5% CO_2 with passages every 2–3 days. Mouse glomerular endothelial cells were maintained in DMEM containing 1,000 mg/l glucose supplemented with 10% FBS.

RT-PCR. Total RNA was isolated from kidney tissues using TRIzol Reagent (Takara) according to the manufacturer's instructions. Total RNA (0.5 μg) was reverse transcribed using 1 μg oligo dT primer with Moloney murine leukemia virus reverse transcriptase (Toyobo) in a 20-μl reaction volume containing 1.25 mM dNTP at 42°C. PCR was performed using 1 μl of cDNA in 20 μl of PCR buffer containing 15 pmol of each primer, 0.1 mM of dNTP, and 0.3 units of *Taq* polymerase (Promega, Shanghai, China). The following primer sequences were used: MAD2B, sense 5′-CGAGTTCCTGGAGGTGGCTGTGCATC-3′ and antisense 5′-CTTGACGCAGTGCAGCGTGTCCTGGATA-3′; and GAPDH, sense 5′-AGGTCGGAGTCAACGGATTG-3′ and antisense 5′-GTGATGGCATGGACTGTGGT-3′. Conditions of these reactions were as follows: 94°C for 5 min, 94°C for 30 s, 58°C for 60 s, and 72°C for 30 s for 38 cycles (PCR product). Products were electrophoresed through 1% agarose gel.

Immunostaining of kidney sections. To evaluate the abundance and localization of MAD2B within mouse glomeruli, we perform dual immunofluorescent staining in frozen tissue. After fixation, tissue was permeabilized, blocked with 5% donkey serum, and then incubated with rabbit monoclonal anti-MAD2B (1:100, Abcam, Cambridge, MA) and goat anti-synaptopodin antibody (1:40, Santa Cruz Biotechnology, Santa Cruz, CA) overnight at 4°C. After being washed with PBS, slides were incubated with Alexa 488- or Alexa 647-labeled secondary antibodies at room temperature for 1 h. Images were captured by confocal microscopy (Fluoview FV1000, Olympus) at

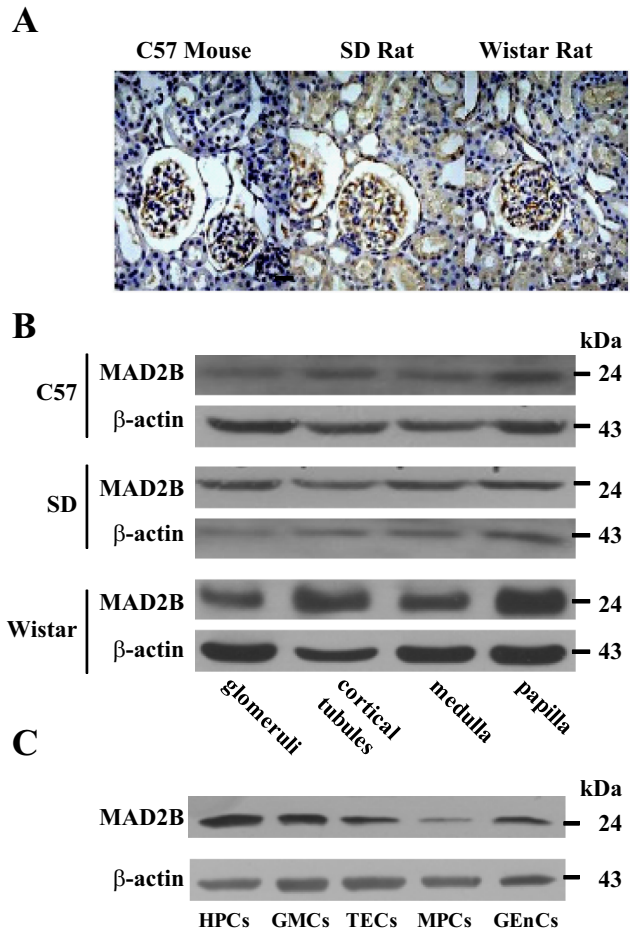

Fig. 1. Expression of mitotic arrest deficiency (MAD)2B in normal kidney tissues and cell lines. *A*: immunohistochemical staining of MAD2B in kidneys of the mouse and rat. Original magnification: ×400. *B*: representative Western blot gel showing relative MAD2B expression in glomeruli, cortical tubules, the medulla, and papilla tissues. *C*: representative Western blot gel showing relative MAD2B expression in renal human podocytes (HPCs), glomerular mesangial cells (GMCs), tubular epithelial cells (TECs), mouse podocytes (MPCs), and glomerular endothelial cells (GEnCs). C57, C57BL/6J mice, SD: Sprague-Dawley rats; Wistar, Wistar rats.

identical microscopic settings. The negative control was set up by replacing primary antibody with PBS, and no visible fluorescence was detected under this condition (data not shown).

Immunohistochemical staining of MAD2B in human renal biopsy samples was performed on formalin-fixed, paraffin-embedded sections. Slides were baked at 60°C for 30 min, deparaffinized with xylenes, and rehydrated in a graded ethanol series to distilled water. Antigen retrieval for MAD2B was performed in microwaved citrate buffer (0.01 M, pH 6.0) for 20 min. Endogenous peroxidase was blocked with 5% BSA in 0.01 M PBS (pH 7.4) for 30 min, and sections were incubated with goat anti-MAD2B antibody (1:300, Rockland, Gilbertsville, PA) overnight at 4°C. Sections were washed in PBS followed by biotinylated anti-goat secondary antibody and avidin-biotin peroxidase complex (Dako, Shanghai, China) for 20 min. After a rinse, peroxidase activity was visualized by diaminobenzidine (Dako), and sections were counterstained with hematoxylin. Negative controls were performed by omitting the primary antibody and replacing it with PBS. Thirty randomly chosen glomeruli were analyzed using Image-pro plus 5.10 software (Media Cybernetics, Rockville, MD) at a magnification of ×400, and integrated optical density was used as the relative amount of positive staining.

Western blot analysis. Immunoblot analysis was performed as previously described (32). Briefly, tissues were lysed in RIPA buffer [50 mM Tris·HCl (pH 8.0), 5 mM EDTA, 150 mM NaCl, 1% Nonidet P-40, 1% Triton X-100, 50 mM NaF, and 1 mM Na-orthovanadate, all from Sigma-Aldrich] with 40 mM protease inhibitor (Roche Molecular Biochemicals, Indianapolis, IN). The protein concentration of cell lysates was measured by a BCA Protein Assay kit (Bio-Rad, Hercules, CA). An equal amount of protein (80 μg) was loaded onto a SDS-polyacrylamide gel (10% polyacrylamide gel) for electrophoresis and then transferred to polyvinylidene difluoride membrane (Merck Millipore, Billerica, MA). The membrane was blocked with 5% fat-free milk solution and then incubated with primary antibodies overnight at 4°C against MAD2B (1:1,000, Rockland), Cdh1 (1:1,000, Abcam), cleaved caspase-3 (1:500, Cell Signaling Technology, Danvers, MA), Skp2 (1:500, Proteintech, Chicago, IL), cyclin B1 (1:500, Proteintech), and desmin (1:800, Proteintech). After an incubation with the appropriate secondary antibodies, signals were visualized by an enhanced chemiluminescence Western blot system. Expression of actin was also assessed as an internal loading control using a specific antibody (1:5,000, Santa Cruz Biotechnology).

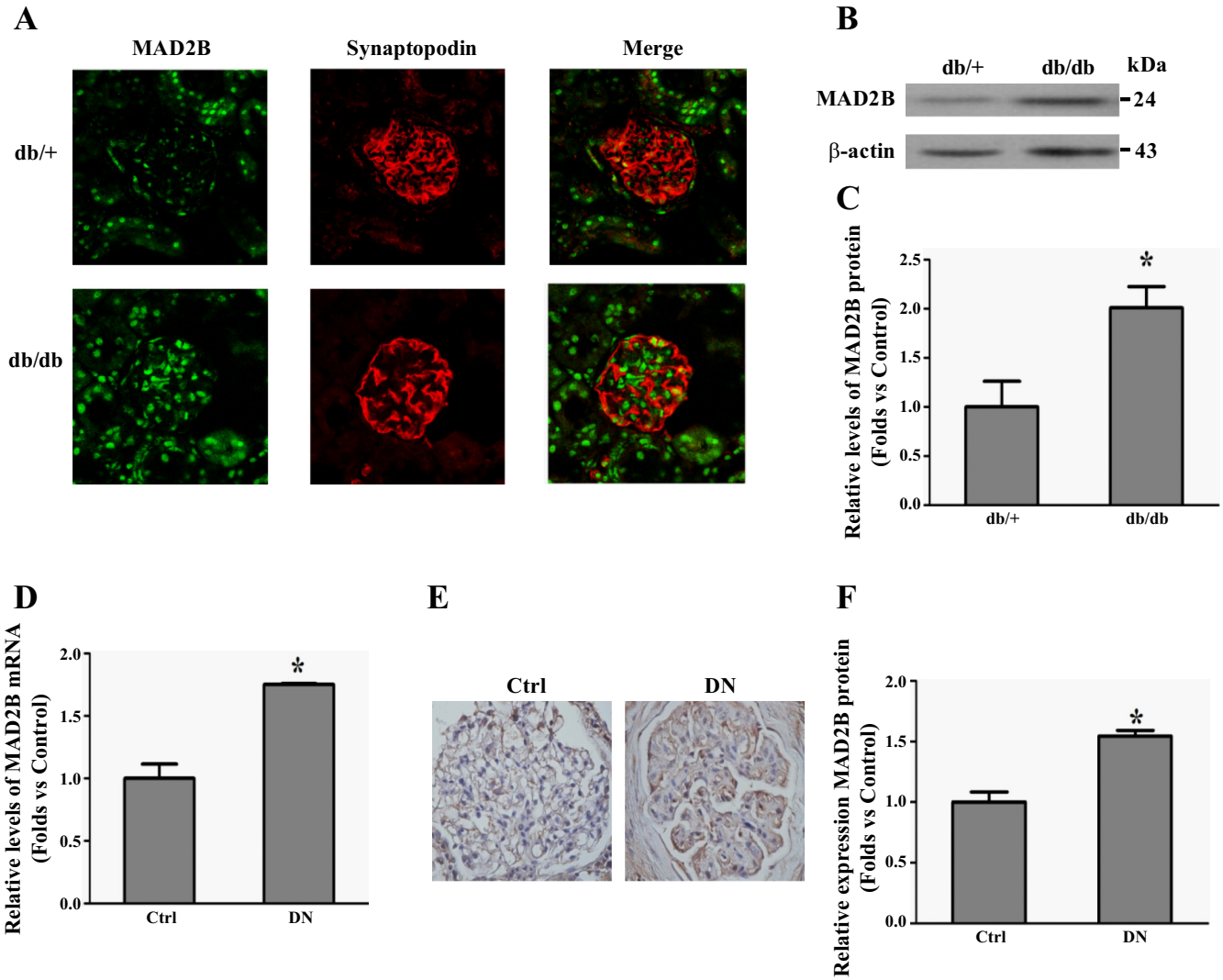

Fig. 2. Abundance of MAD2B in type 2 diabetic nephropathy (DN) mice and humans. *A*: dual immunofluroscence staining of MAD2B and synaptopodin in *db*/+ and *db*/*db* mice. Original magnification: ×400. *B* and *C*: representative Western blot images (*B*) and summarized data (*C*) showing relative MAD2B expression in glomeruli of *db*/*db* and *db*/+ mice. $n = 6$. *$P < 0.05$ vs. *db*/+ mice. *D*: RT-PCR analysis of MAD2B mRNA levels in glomeruli from control (Ctrl) and DN patients. $n = 5–8$. *$P < 0.05$ vs. Ctrl patients. *E* and *F*: immunohistochemical staining (*E*) and summarized data (*F*) of MAD2B levels in glomeruli from Ctrl and DN patients. Original magnification: ×400. $n = 10–12$. *$P < 0.05$ vs. Ctrl patients.

Plasmid DNA and transfections. Transient transfection was carried out using Lipofectamine 2000 according to the manufacturer's protocol (Invitrogen, Grand Island, NY). Briefly, HPCs were seeded at the density of 10^6 cells/60-mm plate overnight and then incubated with serum-free culture medium containing 4 μg pDNA and 10 μl Lipofectamine 2000 for 6 h. Afterward, transfected cells were switched to normal medium for another 12 h before subsequent experiments. In preliminary experiments, almost all cells were positive after transfection with green fluorescent protein (GFP) plasmid, which was detected by fluorescence microscope, demonstrating a high transfection efficiency. The target sequence used for producing rat MAD2B short hairpin (sh)RNA was 5′-GTGTGACATG-TATATATTA-3′, and the scrambled sequence was 5′-TTCTC-CGAACGTGTCACGTTT-3′ (Genchem, Shanghai, China). Plasmids encoding full-length MAD2B were kindly provided by Dr. K. Murakumo (Nagoya University Graduate School of Medicine, Nagoya, Japan). Fragments of the MAD2B open reading frame were amplified and infused into pEGFP-N1 plasmid. pEGFP-N1 plasmid was used as a control for MAD2B transfection.

Cell treatment and grouping. For high glucose treatment, 30.0 mM D-glucose was used. An osmotic control group was set up using 24.4 mM mannitol plus 5.6 mmol/l D-glucose. After being transfected with MAD2B shRNA plasmid for 12 h, HPCs were treated with 30 mM glucose in 3% FBS and DMEM for 48 h and then collected. Forty-eight hours after pEGFP-N1 or pEGFP-N1-MAD2B plasmid transfection, cells were harvested. The cell supernatant was collected to detect lactate dehydrogenase (LDH) activity (assay kit, Cayman Chemical, Ann Arbor, MI). Cells were washed with PBS for subsequent experiments.

Statistical analyses. Statistical differences between treatments were assessed by ANOVA followed by a least-significant-difference multiple-range test. P values of <0.05 were considered significant. Results are expressed as means ± SE.

RESULTS

Characterization of MAD2B expression in normal kidneys and renal cell lines. Immunostaining indicated that MAD2B was expressed in glomerular mesangial cells, endothelial cells, and podocytes as well as proximal tubule epithelial cells of both mice and rats (Fig. 1*A*). Western blot analysis results also

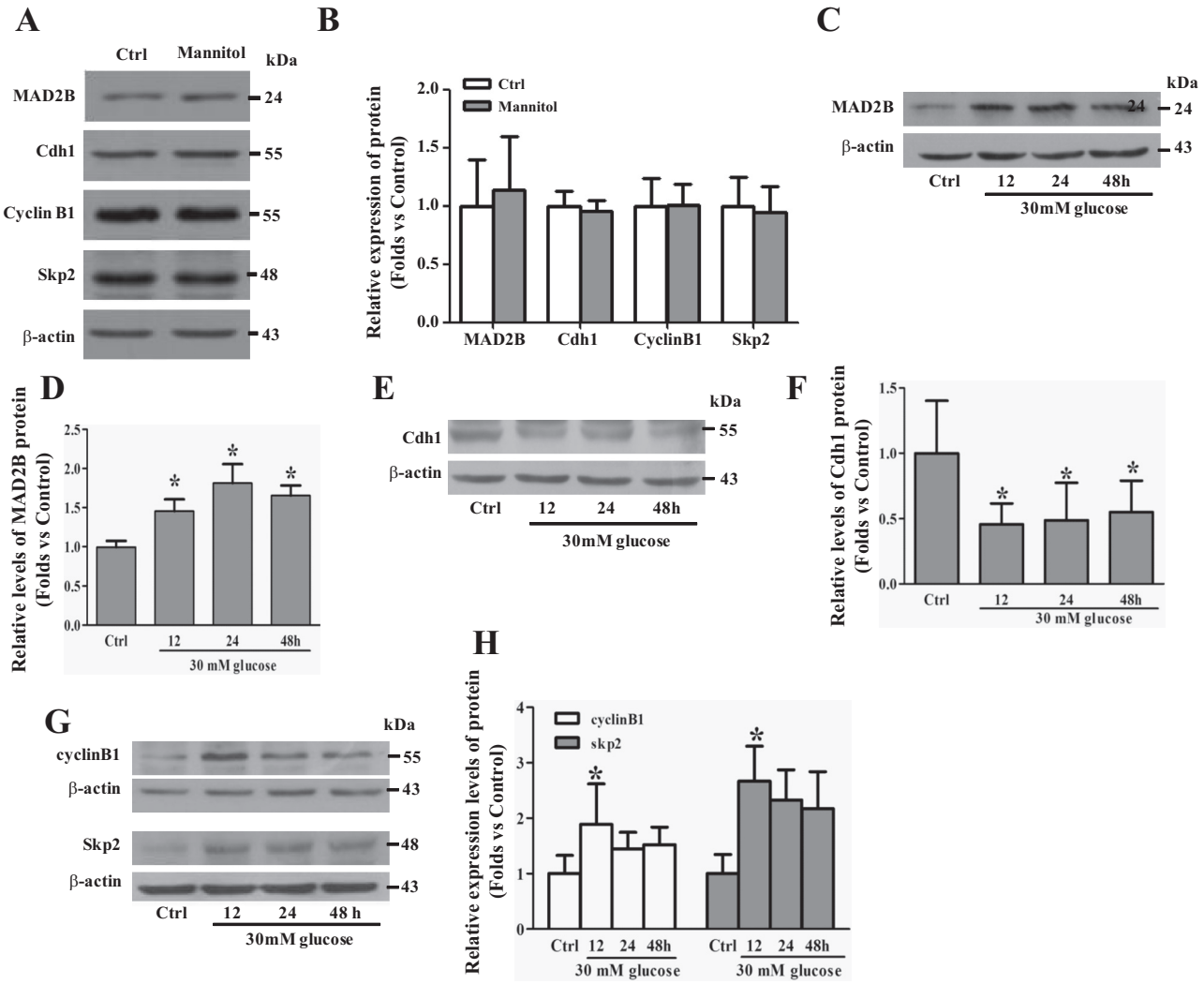

Fig. 3. High glucose regulated the expression of MAD2B, cadherin (Cdh)1, cyclin B1, and S phase kinase-associated protein (Skp)2 in HPCs. *A* and *B*: 24.4 mM mannitol plus 5.6 mmol/l D-glucose was used as an osmotic control. Representative Western blot images (*A*) and summarized data (*B*) indicate that osmotic pressure did not have significant effects on MAD2B, Cdh1, cyclin B1, and Skp2 protein expression. *C* and *D*: representative Western blot images (*C*) and summarized data (*D*) showing that MAD2B expression was upregulated in HPCs with high glucose (30 mM) treatment at various time points. *E* and *F*: representative Western blot images (*E*) and summarized data (*F*) showing that Cdh1 expression was inhibited by high glucose at the indicated time points. *G* and *H*: representative Western blot images (*G*) and summarized data (*H*) showing the abundance of cyclin B1 and Skp2 with high glucose exposure at the indicated time points. $n = 4$. *$P < 0.05$ vs. Ctrl.

suggested that MAD2B was widely expressed in different compartments of the mouse and rat kidney (Fig. 1*B*). Moreover, MAD2B was expressed in various kidney cell lines, including HPCs, glomerular mesangial cells, tubular epithelial cells, mouse podocytes, and glomerular endothelial cells; it was especially highly expressed in HPCs (Fig. 1*C*).

Expression of MAD2B in db/db type 2 diabetic mice and DN patients. Dual immunofluroscence staining was conducted to observe MAD2B changes in glomeruli of 16-wk-old leptin receptor-deficient *db*/*db* mice ($n = 6$) compared with wild-type mice ($n = 6$). Figure 2*A* shows that in glomeruli, MAD2B partially colocalized with the podocyte marker synaptopodin, and the expression of MAD2B was significantly increased in *db*/*db* mice. Western blot analysis results reconfirmed that glomerular MAD2B levels were enhanced in *db*/*db* mice (Fig. 2, *B* and *C*). We also measured mRNA levels of MAD2B by RT-PCR in DN patients ($n = 10$) and normal control subjects ($n = 12$). Compared with normal control subjects, mRNA expression of MAD2B in glomeruli was obviously upregulated in DN patients (Fig. 2*D*). Consistently, by immunohistochemical staining, strong MAD2B nuclear staining was detected in glomeruli of DN patients, whereas only weak staining was observed in glomeruli from control subjects (Fig. 2, *E* and *F*).

High glucose increased MAD2B and decreased Cdh1 expression in human podocytes. First, we found that osmotic pressure did not affect the protein expression of MAD2B and its potential downstream targets (Fig. 3, *A* and *B*). However, as shown in Fig. 3, *C* and *D*, after stimulation with high glucose (30 mM), protein expression of MAD2B was evidently increased in HPCs, as detected by Western blot analysis. As we know that MAD2B regulates APC/C activity via its activator Cdh1, this prompted us to investigate whether high glucose affects Cdh1 expression. As shown in Fig. 3, *E* and *F*, protein levels of Cdh1 were decreased as early as 12 h after high glucose treatment. In addition, both cyclin B1 and Skp2 protein expression were increased with high glucose treatment (Fig. 3, *G* and *H*). The above observation suggests that APC/C activity was inhibited under high glucose in podocytes.

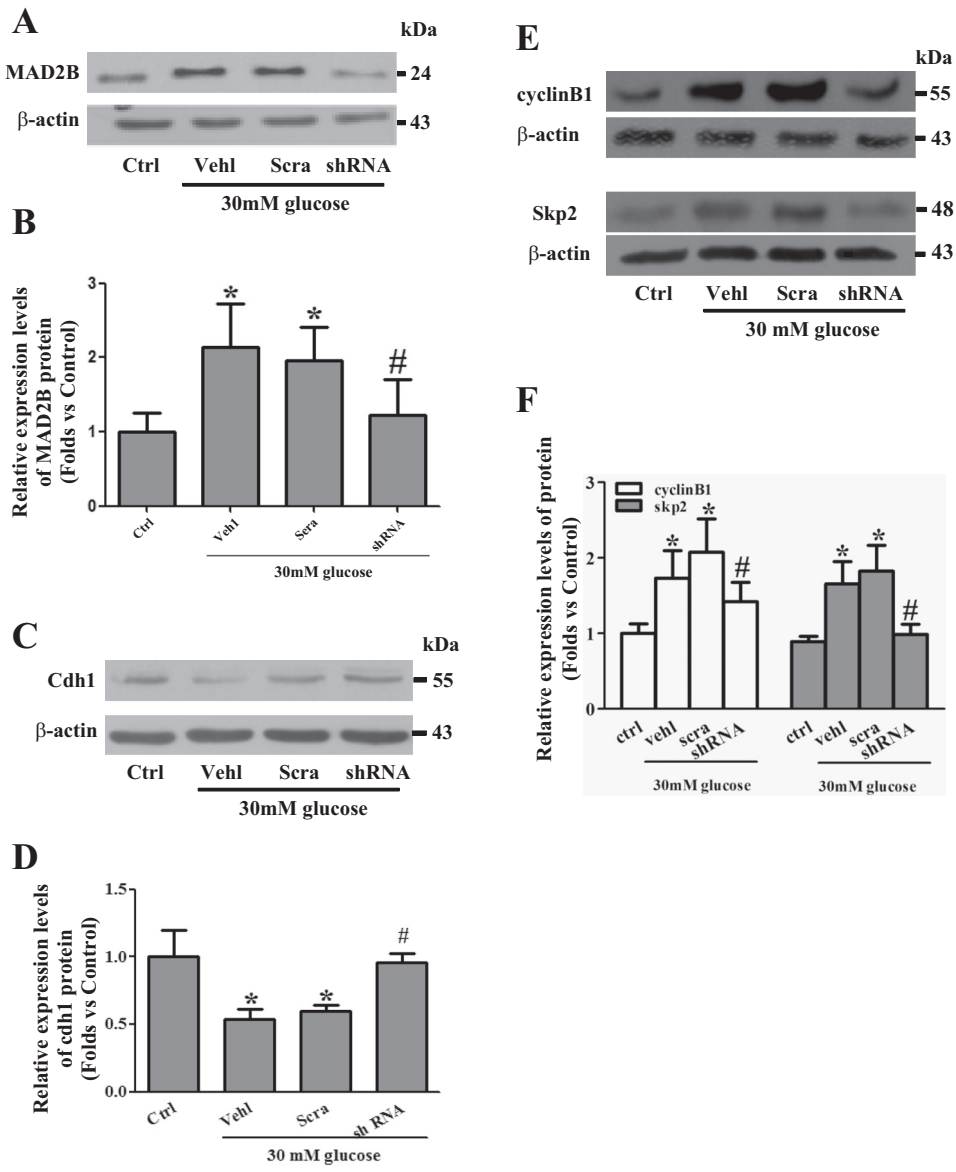

Fig. 4. MAD2B deletion increased Cdh1 abundance and inhibited the expression of cyclin B1 and Skp2 under the high glucose condition. *A* and *B*: MAD2B short hairpin (sh)RNA effectively inhibited high glucose-indcued MAD2B expression in HPCs. *C* and *D*: suppression of MAD2B attenuated the high glucose-induced Cdh1 reduction. *E* and *F*: blockage of MAD2B prevented the accumulation of cyclin B1 and Skp2 in HPCs with high glucose treatment. $n = 4$. Vehl, vehicle; Scra, scrambled shRNA. $^*P < 0.05$ vs. Ctrl; $\#P < 0.05$ vs. the Scra group with high glucose.

MAD2B deficiency suppressed cyclin B1 and Skp2 expression and rescured podocytes impairment induced by high glucose. To evaluate whether MAD2B was responsible for the increased levels of cyclin B1 and Skp2 under hyperglycemia, MAD2B shRNA was used, which could effectively inhibit MAD2B expression (Fig. 4, *A* and *B*). We found MAD2B gene silencing attenuated the reduction in Cdh1 and suppressed the increases in cyclin B1 and Skp2 induced by high glucose in podocytes, as detected by Western blot analysis (Fig. 4, *C–F*).

Next, we analyzed the effect of high glucose on cell viability. By detecting LDH activity, we found that high glucose significantly decreased the viability of podocytes (Fig. 5*A*). Levels of cleaved caspase-3, an active executioner caspase and apoptosis marker, were obviously upregulated with high glucose stimulation, suggesting that high glucose prompted podocyte apoptosis (Fig. 5, *B* and *C*). To further explore the role of MAD2B in high glucose-induced podocyte injury, we transfected MAD2B shRNA into podocytes. We found that knockdown of MAD2B attenuated high glucose-induced cellular injury and apoptosis, as detected by LDH activity and levels of cleaved caspase-3 (Fig. 5, *D–F*). Additionally, the expression of desmin, a marker of podocyte damage, was analyzed by Western blot analysis. Our data showed that desmin was markedly suppressed with MAD2B deletion (Fig. 5, *G* and *H*). Taken together, these data suggested that silencing of MAD2B ameliorated high glucose-induced podocyte injury.

Overexpression of MAD2B increased cyclin B1 and Skp2 abundance and led to podocyte injury. Finally, we found that overexpression of MAD2B in podocytes by plasmid transfection suppressed Cdh1 expression, whereas it enhanced the expression of cyclin B1 and Skp2 (Fig. 6, *A–E*). Additionally, upregulation of MAD2B led to podocyte dysfunction along with higher LDH activity as well as increased levels of cleaved caspase-3 and desmin (Fig. 6, *F–I*), which was consistent with our observations in high glucose-stimulated podocytes.

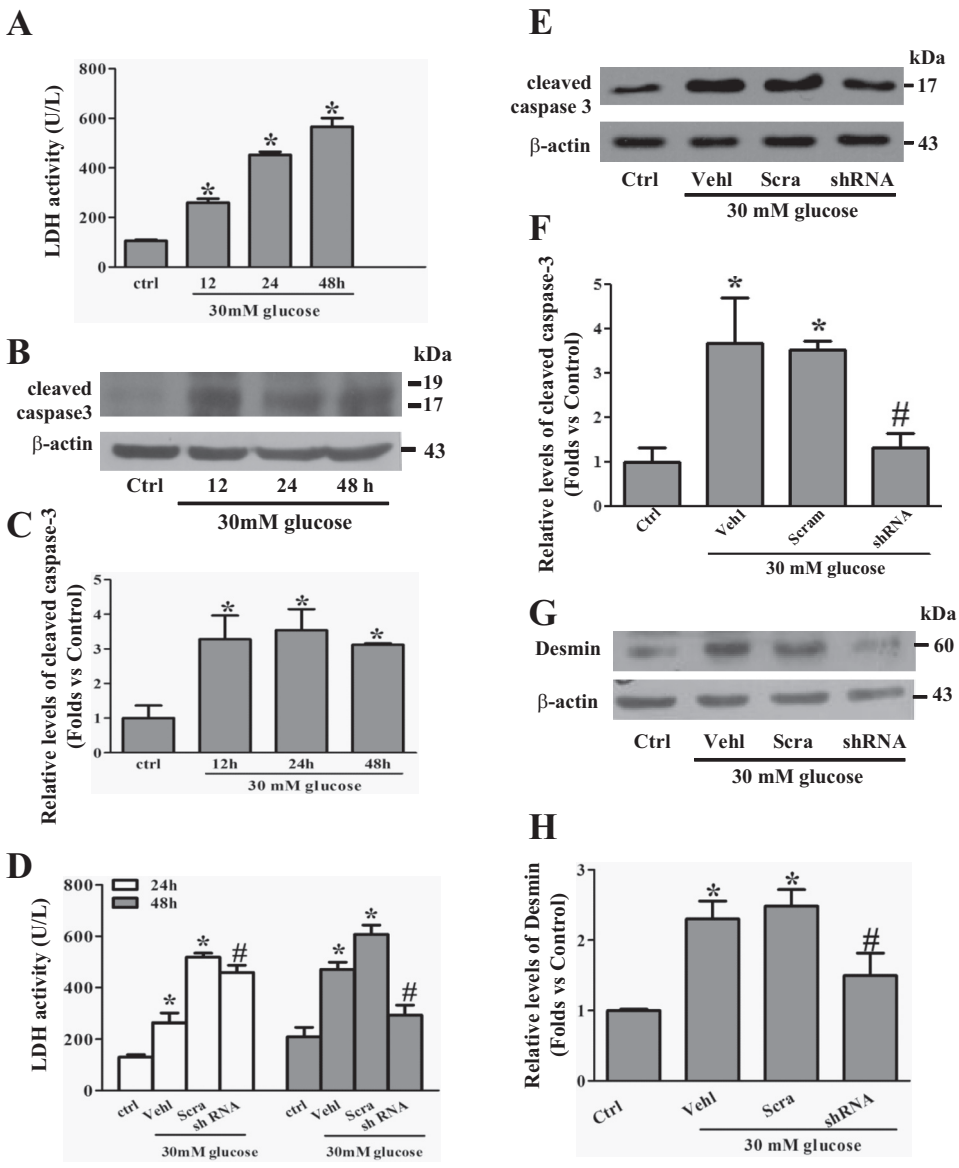

Fig. 5. MAD2B deficiency ameliorated podocyte injury induced by high glucose. *A*: LDH activity of HPCs with high glucose exposure at the indicated time points. *B* and *C*: representative Western blot images (*B*) and summarized data (*C*) showing cleaved caspase-3 expression with high glucose treatment at the indicated time points. *D*: MAD2B gene silencing inhibited LDH activity under high glucose status. *E* and *F*: representative Western blot images (*E*) and summarized data (*F*) showing that the abundance of cleaved caspase-3 was decreased in MAD2B-deficient HPCs under high glucose status. *G* and *H*: representative Western blot images (*G*) and summarized data (*H*) showing that the expression of desmin was reduced in MAD2B-deficient podocytes stimulated by high glucose. $n = 4$. $^*P < 0.05$ vs. Ctrl; $\#P < 0.05$ vs. the Scra group with high glucose.

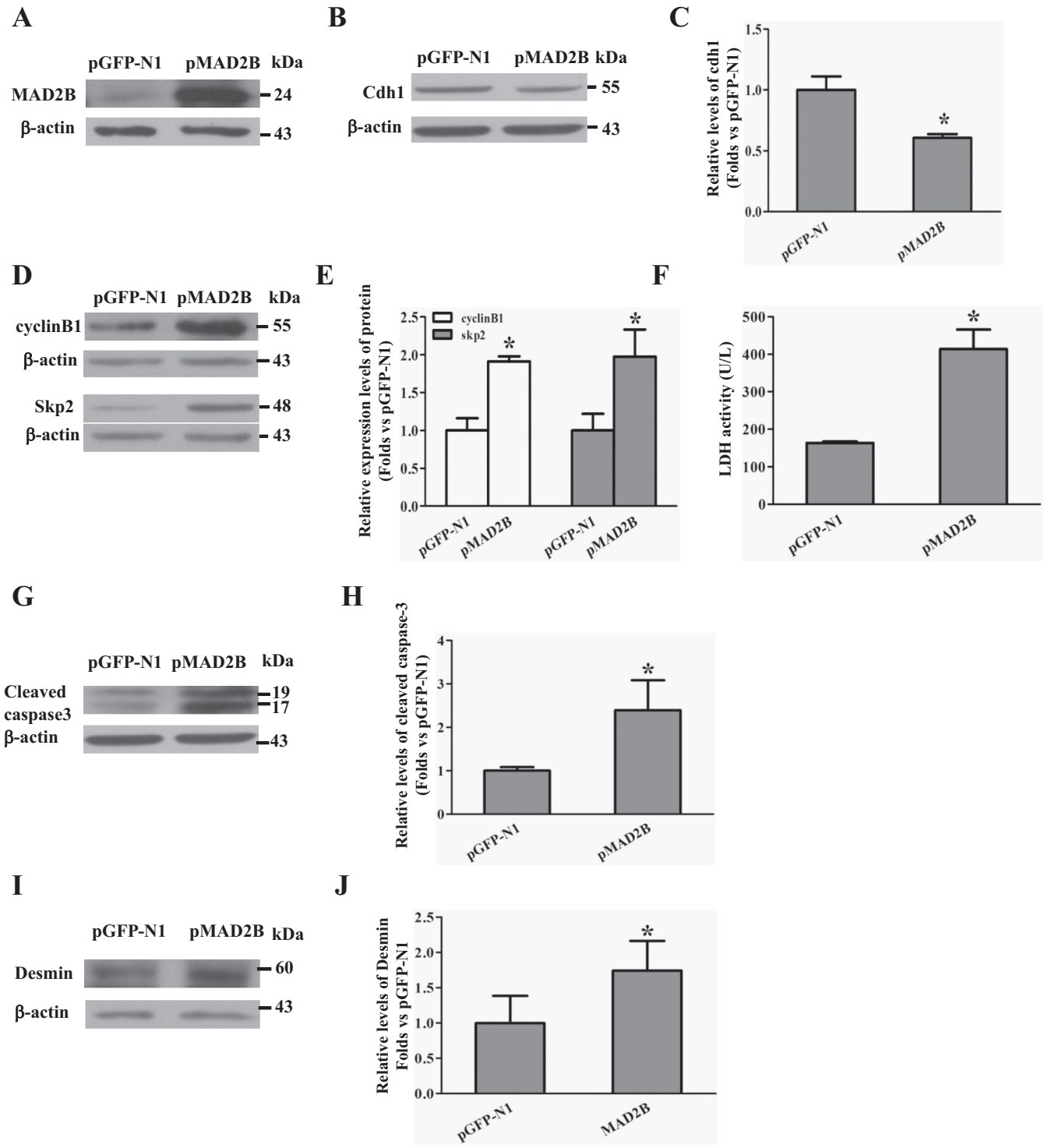

Fig. 6. Overexpression of MAD2B reduced the abundance of Cdh1 and upregulated cyclin B1 and Skp2, which finally resulted in podocyte injury. *A*: Western blots showing that MAD2B plasmids were successfully expressed in HPCs. *B* and *C*: overexpression of MAD2B dampened the expression of Cdh1. *D* and *E*: overexpression of MAD2B induced anaphase-promoting complex/cyclosome substrate cyclin B1 and Skp2 accumulation in HPCs. *F*: LDH activity in HPCs with or without MAD2B gene overexpression. *G* and *H*: representative Western blot images (*G*) and normalized data (*H*) showing the expression of cleaved caspase-3 in HPCs transfected with pEGFP-N1 or pEGFP-MAD2B. *I* and *J*: desmin expression in podocytes with or without MAD2B gene overexpression. $n = 4$. *$P < 0.05$ vs. the pEGFP-N1 group.

DISCUSSION

In the present study, we elucidated that MAD2B was upregulated in kidneys of human and mice with DN. Genetic ablation of MAD2B by shRNA attenuated the extent of podocyte impairment induced by high glucose. These results suggest that MAD2B has a potential role in DN. In the mitotic cell cycle, APC/C is activated at the onset of anaphase, and its activity persists through most of the G_1 phase (4, 5, 8). The

activity of APC/C is controlled by a network of regulatory factors, including MAD2B. MAD2B is the human homolog of yeast Rev7 and shares 53% similarity with human MAD2 (also known as MAD2L1), a key mitotic checkpoint protein (5) that has been shown to inhibit activity of the cell cycle regulator Cdh1-APC/C. However, the role of MAD2B in human kidney diseases, including DN, remains unclear.

Here, we first identified that MAD2B was expressed in kidneys from the human, mouse, and rat and distributed in glomeruli, tubules, the medulla, and papillary tissues. Furthermore, by Western blot analysis, we found that MAD2B was also expressed in cultured podocytes and glomerular mesangial and endothelial cells as well as tubular epithelial cell lines. These results suggest that MAD2B is expressed widely in kidneys and potentially plays an important role under physiological conditions. In the present study, we explored the underlying role of MAD2B in DN. By Western blot analysis and immunohistochemistry, we demonstrated that MAD2B was upregulated in kidneys from *db*/*db* mice and in DN patients as well. These findings suggested that MAD2B may be implicated in the pathogenesis of DN.

It is well recognized that the foot process effacement of podocytes, one of the earliest abnormalities of DN, largely contributes to albuminuria development (9). Therefore, we investigated the involvement of MAD2B-mediated signaling in podocyte abnormalities. When podocytes were stimulated by high glucose, the expression of MAD2B was gradually increased. Given that MAD2B was upregulated in podocytes under hyperglycemia and its role in mitotic checkpoint control, we hypothesized that MAD2B could affect the expression of APC/C regulatory molecules, including substrates of APC/C. In this regard, we examined the expression of Cdh1, one of the APC/C regulators, under hyperglycemia. As expected, Cdh1 expression began to decrease after 12 h of exposure to high glucose. We then assessed the abundance of substrates of APC/C, including cyclin B1 and Skp2. Cyclin B1 is involved in checkpoint control, and increasing numbers of studies have demonstrated its role in various malignant diseases (11, 17). In addition, it has also been found that nuclear accumulation of cyclin B1 is a signal for apoptotic initiation (3). Moreover, upregulation of Skp2 may lead to cell cycle progression in a variety of cancers (10), and Skp2 is a key molecule involved in renal injury in the unilateral ureteral obstruction model (25). Under high glucose conditions, we found that Cdhl-APC/C was inhibited by upregulated MAD2B and that its substrates, which are degraded via ubiquitinated modification, including cyclin B1 and Skp2, had accumulated. The increased levels of cyclin B1 and Skp2 might lead to podocyte injury. Podocyte injury was analyzed by measuring LDH activity, apoptosis protein cleaved caspase-3, and desimin expression. Our data showed that high glucose induced MAD2B upregulation and eventually led to podocyte injury.

To assess whether MAD2B was directly responsible for podocyte damage, we used shRNA specifically targeted against MAD2B. We found that genetic inhibition of MAD2B increased the survival of podocytes under high glucose by preventing cyclin B1 and Skp2 accumulation. Consistently, MAD2B gene silencing alleviated podocytes impairment, as evaluated by cleaved caspase-3 and desmin. Conversely, overexpression of MAD2B aggravated cell injury compared with control cells. It has been shown that Cdk1/cyclin B1 could mediate cell death by catalyzing Bcl-2-associated death promoter protein phosphorylation (12) and that overexpression of Skp2 may lead to cell cycle progression (14). In this sense, our data suggest that nuclear localization of cyclin B1 and accumulation of Skp2 are downstream events of high glucose-induced MAD2B upregulation that directly contributed to podocyte injury.

Taken together, in the present study, we demonstrated that MAD2B is upregulated in kidneys of DN patients and a mouse model. In addition, we observed that MAD2B overexpression deteriorates podocyte impairment, whereas knockdown of MAD2B protects against high glucose-induced podocyte injury. Furthermore, we propose that enhanced MAD2B could dampen Cdhl-APC/C-driven cyclin B1 and Skp2 degradation and consequently initiates an aberrant reentry into the cell cycle in podocytes. Hence, our observations suggest that MAD2B may be a new target for early intervention in DN.

GRANTS

This work was supported by National Natural Science Foundation of China Grants 30871174, 81170662, 81170600, 31200872, 81300604, 81470964, 81400720, and 81471490, Natural Science Foundation of Hubei Province Grants 2013CFA026 and 2012FFA038, Doctoral Fund of Ministry of Education of China Grant 20130142110064, and Fundamental Research Funds for the Central Universities Grant 2013QN176. Editorial assistance was provided by Rebecca Lew, PhD, of ProScribe Medical Communications (www.proscribe.com.au) and was funded by Baxter Healthcare. Baxter Healthcare did not sponsor this study. In compliance with the International Committee of Medical Journal Editors Recommendations, Baxter Healthcare did not influence the study design, data collection/analysis, or decision to publish this manuscript. ProScribe's services complied with international guidelines for Good Publication Practice (GPP2).

DISCLOSURES

No conflicts of interest, financial or otherwise, are declared by the author(s).

AUTHOR CONTRIBUTIONS

Author contributions: H.S., Q.W., and F.-F.H. prepared figures; H.S., Q.W., and F.-F.H. drafted manuscript; X.-J.T., H.T., and C.Y. performed experiments; P.G., D.F., S.C., and Y.-M.W. analyzed data; X.-F.M. and C.Z. conception and design of research; X.-F.M. and C.Z. approved final version of manuscript.

REFERENCES

1. **Ali IH, Brazil DP.** Under the right conditions: protecting podocytes from diabetes-induced damage. *Stem Cell Res Ther* 4: 119, 2013.
2. **Almeida A.** Regulation of APC/C-Cdh1 and its function in neuronal survival. *Mol Neurobiol* 46: 547–554, 2012.
3. **Almeida A, Bolanos JP, Moreno S.** Cdh1/Hct1-APC is essential for the survival of postmitotic neurons. *J Neurosci* 25: 8115–8121, 2005.
4. **Amon A, Irniger S, Nasmyth K.** Closing the cell cycle circle in yeast: G2 cyclin proteolysis initiated at mitosis persists until the activation of G1 cyclins in the next cycle. *Cell* 77: 1037–1050, 1994.
5. **Cahill DP, da Costa LT, Carson-Walter EB, Kinzler KW, Vogelstein B, Lengauer C.** Characterization of MAD2B and other mitotic spindle checkpoint genes. *Genomics* 58: 181–187, 1999.
6. **Chen J, Fang G.** MAD2B is an inhibitor of the anaphase-promoting complex. *Genes Dev* 15: 1765–1770, 2001.
7. **Eguren M, Manchado E, Malumbres M.** Non-mitotic functions of the anaphase-promoting complex. *Semin Cell Dev Biol* 22: 572–578, 2011.
8. **Fang G, Yu H, Kirschner MW.** Direct binding of CDC20 protein family members activates the anaphase-promoting complex in mitosis and G1. *Mol Cell* 2: 163–171, 1998.
9. **Gruden G, Perin PC, Camussi G.** Insight on the pathogenesis of diabetic nephropathy from the study of podocyte and mesangial cell biology. *Curr Diabetes Rev* 1: 27–40, 2005.

10. **Gstaiger M, Jordan R, Lim M, Catzavelos C, Mestan J, Slingerland J, Krek W.** Skp2 is oncogenic and overexpressed in human cancers. *Proc Natl Acad Sci USA* 98: 5043–5048, 2001.
11. **Jain P, Baranwal S, Dong S, Struckhoff AP, Worthylake RA, Alahari SK.** Integrin-binding protein nischarin interacts with tumor suppressor liver kinase B1 (LKB1) to regulate cell migration of breast epithelial cells. *J Biol Chem* 288: 15495–15509, 2013.
12. **Konishi Y, Lehtinen M, Donovan N, Bonni A.** Cdc2 phosphorylation of BAD links the cell cycle to the cell death machinery. *Mol Cell* 9: 1005–1016, 2002.
13. **Kramer ER, Scheuringer N, Podtelejnikov AV, Mann M, Peters JM.** Mitotic regulation of the APC activator proteins CDC20 and CDH1. *Mol Biol Cell* 11: 1555–1569, 2000.
14. **Langner C, von Wasielewski R, Ratschek M, Rehak P, Zigeuner R.** Biological significance of p27 and Skp2 expression in renal cell carcinoma. A systematic analysis of primary and metastatic tumour tissues using a tissue microarray technique. *Virchows Arch* 445: 631–636, 2004.
15. **Lasagni L, Lazzeri E, Shankland SJ, Anders HJ, Romagnani P.** Podocyte mitosis–a catastrophe. *Curr Mol Med* 13: 13–23, 2013.
16. **Listovsky T, Sale JE.** Sequestration of CDH1 by MAD2L2 prevents premature APC/C activation prior to anaphase onset. *J Cell Biol* 203: 87–100, 2013.
17. **Pandey JP, Namboodiri AM, Kistner-Griffin E.** A genetic variant of FcgammaRIIIa is strongly associatedwith humoral immunity to cyclin B1 in African American patients with prostate cancer. *Immunogenetics* 65: 91–96, 2013.
18. **Peters JM.** The anaphase promoting complex/cyclosome: a machine designed to destroy. *Nat Rev Mol Cell Biol* 7: 644–656, 2006.
19. **Pfleger CM, Salic A, Lee E, Kirschner MW.** Inhibition of Cdh1-APC by the MAD2-related protein MAD2L2: a novel mechanism for regulating Cdh1. *Genes Dev* 15: 1759–1764, 2001.
20. **Pirouz M, Pilarski S, Kessel M.** A critical function of Mad2l2 in primordial germ cell development of mice. *PLoS Genet* 9: e1003712, 2013.
21. **Reddy GR, Kotlyarevska K, Ransom RF, Menon RK.** The podocyte and diabetes mellitus: is the podocyte the key to the origins of diabetic nephropathy? *Curr Opin Nephrol Hypertens* 17: 32–36, 2008.
22. **Sanchez-Nino MD, Sanz AB, Sanchez-Lopez E, Ruiz-Ortega M, Benito-Martin A, Saleem MA, Mathieson PW, Mezzano S, Egido J, Ortiz A.** HSP27/HSPB1 as an adaptive podocyte antiapoptotic protein activated by high glucose and angiotensin II. *Lab Invest* 92: 32–45, 2012.
23. **Shankland SJ.** The podocyte's response to injury: role in proteinuria and glomerulosclerosis. *Kidney Int* 69: 2131–2147, 2006.
24. **Susztak K, Raff AC, Schiffer M, Bottinger EP.** Glucose-induced reactive oxygen species cause apoptosis of podocytes and podocyte depletion at the onset of diabetic nephropathy. *Diabetes* 55: 225–233, 2006.
25. **Suzuki S, Fukasawa H, Misaki T, Togawa A, Ohashi N, Kitagawa K, Kotake Y, Niida H, Hishida A, Yamamoto T, Kitagawa M.** Up-regulation of Cks1 and Skp2 with TNFα/NF-κB signaling in chronic progressive nephropathy. *Genes Cells* 16: 1110–1120, 2011.
26. **Tamura K, Ono A, Miyagishima T, Nagao T, Urushidani T.** Comparison of gene expression profiles among papilla, medulla and cortex in rat kidney. *J Toxicol Sci* 31: 449–469, 2006.
27. **Thornton BR, Toczyski DP.** Precise destruction: an emerging picture of the APC. *Genes Dev* 20: 3069–3078, 2006.
28. **Thornton BR, Toczyski DP.** Securin and B-cyclin/CDK are the only essential targets of the APC. *Nat Cell Biol* 5: 1090–1094, 2003.
29. **Wolf G, Chen S, Ziyadeh FN.** From the periphery of the glomerular capillary wall toward the center of disease: podocyte injury comes of age in diabetic nephropathy. *Diabetes* 54: 1626–1634, 2005.
30. **Yeong FM, Lim HH, Padmashree CG, Surana U.** Exit from mitosis in budding yeast: biphasic inactivation of the Cdc28-Clb2 mitotic kinase and the role of Cdc20. *Mol Cell* 5: 501–511, 2000.
31. **Zhang C, Hu JJ, Xia M, Boini KM, Brimson CA, Laperle LA, Li PL.** Protection of podocytes from hyperhomocysteinemia-induced injury by deletion of the gp91^{phox} gene. *Free Radic Biol Med* 48: 1109–1117, 2010.
32. **Zhang C, Yi F, Xia M, Boini KM, Zhu Q, Laperle LA, Abais JM, Brimson CA, Li PL.** NMDA receptor-mediated activation of NADPH oxidase and glomerulosclerosis in hyperhomocysteinemic rats. *Antioxid Redox Signal* 13: 975–986, 2010.
33. **Zou AP, Billington H, Su N, Cowley AW Jr.** Expression and actions of heme oxygenase in the renal medulla of rats. *Hypertension* 35: 342–347, 2000.